Analysis of Linear Noisy Two-Ports Using Scattering Waves

RUDOLF P. HECKEN

In honor of Prof. H. Döring (Aachen, W. Germany) who celebrated his 70th birthday in 1981

Abstract—**This paper proposes a new approach to the use of scattering waves for spot noise analysis of linear N-ports. Noise as a stationary, stochastic process is approximated by an infinite series of partial noise waves. This allows the use of the scattering matrix formalism and signal flowgraph theory. The noise waves lead to a new set of three dimensionless, characteristic noise parameters. Methods to determine these parameters are simple. With these parameters, the theory of noise minimization is straightforward and the definition of constant noise circles uncomplicated. The effect of losses in noise matching networks is shown to be more significant in very low noise amplifiers than usually assumed.**

I. Introduction

THE THEORY OF noisy, linear two-ports is well established and has provided the basis for optimizing the performance of low-noise amplifiers. Especially in the microwave frequency range, this theory is very powerful in design and evaluation of devices and amplifiers. The representation of spot noise[1] in terms of scattering waves is not new [2]–[4], [7] but the theory has been based on the classical work by Rothe and Dahlke [1] who arrive at an impedance or admittance representation of noise parameters. In this paper we will present briefly, an independent derivation of noise waves based on terminal voltages and currents as stationary stochastic processes. This approach leads to a new set of characteristic noise parameters and to simple methods of determining them experimentally. With these parameters, the theory of minimizing amplifier noise by noise matching is straightforward, and the definition of constant noise circles [8] in the Smith chart is very simple. Moreover, it is shown that even small resistive losses in matching networks can significantly increase the noise figure of amplifiers using very low-noise microwave GaAs FET's.

First we deal with the derivation of spot noise waves and the formulation of scattered noise waves for linear N-ports. This theory is then applied to the single complex impedance and to the linear, noisy two-port (Sections IV and V). This leads us to the familiar circles of constant noise factor (Section VI) and to the theory of noise minimization (Section VII). In Sections VIII and IX, we explain a simple measurement method of the noise parameters and investigate the effect of losses in matching networks on the optimum noise figure.

Manuscript received February 24, 1981; revised June 3, 1981.

The author is with Bell Laboratories, North Andover, MA 01845.

[1]The term "spot noise" is used here in accordance with the definition in [6].

II. Noise Waves as Stationary Stochastic Processes

The terminal voltages and currents at an arbitrary port of a linear N-port are defined in Fig. 1. We assume both as stationary stochastic processes and form two new processes defined by the linear transformation

$$a(t)=\tfrac{1}{2}(v(t)+Zi(t))/\sqrt{Z} \tag{1a}$$

$$b(t)=\tfrac{1}{2}(v(t)-Zi(t))/\sqrt{Z} \tag{1b}$$

where Z is a time-independent normalizing quantity with the dimension of an impedance. It is well known that $v(t)$ and $i(t)$ can be approximated by the series [5]

$$v(t)\cong\frac{1}{\sqrt{2}}\sum_{n=-\infty}^{+\infty}V_n e^{jn\Delta\omega t} \tag{2a}$$

and

$$i(t)\cong\frac{1}{\sqrt{2}}\sum_{n=-\infty}^{+\infty}I_n e^{jn\Delta\omega t} \tag{2b}$$

with the complex coefficients V_n and I_n being orthogonal and uncorrelated, i.e., $E\{V_nV_m^*\}=0$ and $E\{I_nI_m^*\}=0$ for $n\neq m$, where $E\{\cdot\}$ denotes statistical expectation. The approximation can be made arbitrarily close by letting $\Delta\omega$ approach zero. Combining (2) with (1) shows that $a(t)$ and $b(t)$ are then also approximated by two series of the same form

$$a(t)\cong\frac{1}{\sqrt{2}}\sum_{n=-\infty}^{+\infty}A_n e^{jn\Delta\omega t} \tag{3a}$$

and

$$b(t)\cong\frac{1}{\sqrt{2}}\sum_{n=-\infty}^{+\infty}B_n e^{jn\Delta\omega t} \tag{3b}$$

where the coefficients A_n and B_n are related to the V_n and I_n by

$$A_n=\tfrac{1}{2}(V_n+ZI_n)/\sqrt{Z} \tag{4a}$$

$$B_n=\tfrac{1}{2}(V_n-ZI_n)/\sqrt{Z}\,. \tag{4b}$$

They are, therefore, also complex, orthogonal, and uncorre-

0018-9480/81/1000-0997$00.75

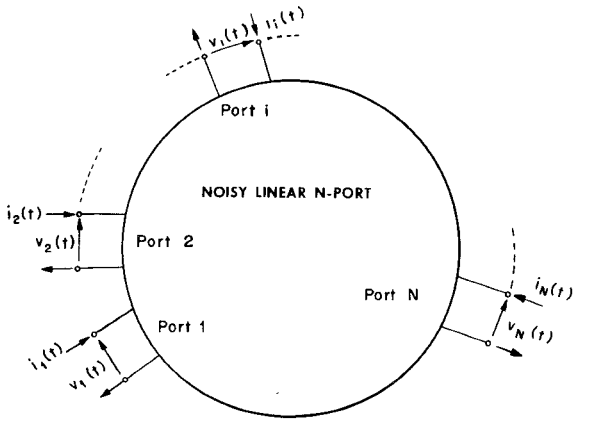

Fig. 1. Definition of currents and voltages of a linear N-port.

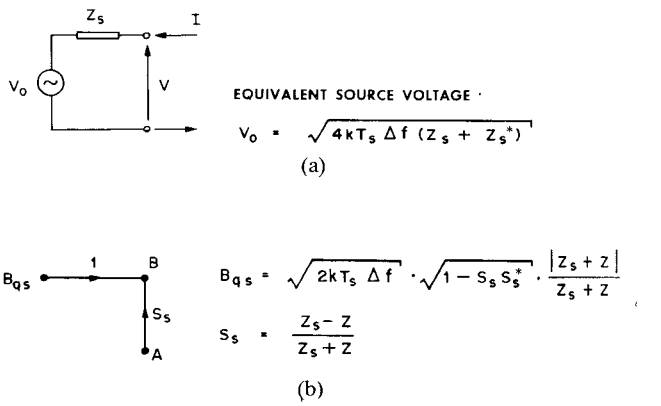

Fig. 2. Noise waves of a complex impedance. (a) Definition of source voltage. (b) Signal flowgraph of the one-port noise source.

lated: $E\{A_n A_m^*\}$ and $E\{B_n B_m^*\}=0$ for $n\neq m$. Equation (4) is identical to the standard definition of scattered waves for sinusoidal processes. According to (3), $a(t)$ and $b(t)$ can, therefore, be interpreted as two processes which consist of an infinite sum of scattered noise waves with complex amplitudes A_n and B_n located on the frequency axis at $n\cdot\Delta\omega$. The noise properties of a linear N-port can thus be studied at any frequency spot $n\cdot\Delta\omega$ using the scattering matrix formalism developed for single-frequency excitation.

III. Noise Analysis with the Scattering Matrix

In the following, we will introduce the new notation $A=A_n=A(n\Delta\omega)$ and $B=B_n=B(n\Delta\omega)$, thus omitting the subscript n. It is well known that for a linear N-port the departing wave B_i at an arbitrary port i ($i=1,2,\cdots,N$) is related to all incident waves A_j ($j=1,2,\cdots,N$) through the scattering coefficients S_{ij}, evaluated in our case at $n\cdot\Delta\omega$. However, because of inherent noise sources in the noisy N-port, we have to assume that in general all departing noise waves will contain components which are independent of all incident waves. Denoting this independent, departing noise wave at port i by B_{qi}, the complete set of linear equations relating the noise waves can be written as

$$\begin{aligned} B_1 &= S_{11}A_1 + S_{12}A_2 + \cdots S_{1N}A_N + B_{q1} \\ B_2 &= S_{21}A_1 + S_{22}A_2 + \cdots S_{2N}A_N + B_{q2} \\ &\vdots \\ B_N &= S_{N1}A_1 + S_{N2}A_2 + \cdots S_{NN}A_N + B_{qn}. \end{aligned} \tag{5}$$

In matrix notation (5) is written as

$$[B]=[S]\cdot[A]+[B_q]. \tag{6}$$

$[A]$, $[B]$, and $[B_q]$ are N-element column matrices, and $[S]$ is an $N\times N$ square matrix. In general all wave sources are correlated.

IV. Application to a Single Complex Impedance

In the case of a single complex impedance Z_s, used as a one-port as shown in Fig. 2a, (5) reduces to

$$B=S_s\cdot A+B_{qs} \tag{7}$$

with S_s being the internal reflection coefficient

$$S_s=\frac{Z_s-Z}{Z_s+Z} \tag{8}$$

and Z the normalizing impedance as before. From Nyquist's theorem [5] we know that the open-circuit noise voltage at the terminals is given by

$$V_o=\sqrt{2}\sqrt{2kT_s\Delta f\cdot(Z_s+Z_s^*)} \tag{9}$$

where Z_s^* is the complex conjugate of Z_s, k the Boltzmann constant, T_s the absolute temperature of the impedance, and Δf the effective bandwidth. (The factor $\sqrt{2}$ stems from the definition of the complex coefficients in (2) and (3) as "peak values.") Applying the transformation (4) to the terminal quantities V and I yields for the equivalent noise wave

$$B_{qs}=\sqrt{2kT_s\Delta f}\cdot\sqrt{1-S_sS_s^*}\,\frac{|Z_s+Z|}{Z_s+Z}. \tag{10}$$

Fig. 2(b) shows a signal flowgraph representation of the complex impedance. Note that the average power in the departing noise wave B_{qs} is given by

$$p_d=\tfrac{1}{2}E\{B_{qs}B_{qs}^*\}=kT_s\Delta f(1-|S_s|^2). \tag{11}$$

Terminating the one-port with an impedance Z_L at $T=0$ K yields the relations

$$A=\rho_L\cdot B \tag{12}$$

and

$$B=\frac{B_{qs}}{1-\rho_L S_s} \tag{13}$$

where ρ_L is the terminating reflection coefficient

$$\rho_L=\frac{Z_L-Z}{Z_L+Z}. \tag{14}$$

The noise power absorbed in Z_L is thus given by

$$p_{\text{abs}}=\tfrac{1}{2}E\{BB^*\}-\tfrac{1}{2}E\{AA^*\}$$

or with (11), (12), and (13)

$$p_{\text{abs}}=kT_s\Delta f\frac{(1-S_sS_s^*)(1-\rho_L\rho_L^*)}{(1-S_s\rho_L)(1-S_s^*\rho_L^*)}. \tag{15}$$

The maximum available noise power $kT_s\Delta f$ is delivered to the "cold" load Z_L if $\rho_L = S_s^*$ or $Z_L = Z_s^*$.

V. The Noise Factor of a Linear Noisy Two-Port

A case of great interest to the design engineer is the noise analysis of linear amplifiers. A basic circuit is shown in Fig. 3. In this configuration, the active, linear two-port is connected via a lossless "noise matching network" to a source with impedance Z_s at standard temperature T_0 and terminated with a cold[2] load impedance Z_L. The analysis is simplified by using signal flow graphs as shown in Fig. 3(b). Here the S_{ij}^0 are the scattering coefficients of the matching network and the S_{ij} those of the active two-port as given by (5) with $N=2$. S_s and ρ_L are the reflection coefficients of the source and load, respectively. We will assume further that the source impedance Z_s and the load impedance Z_L are purely resistive and equal to the normalizing impedance Z. This simplifies the discussion and corresponds to the practical situation in which device and network parameters are determined under well-matched, specific impedance conditions. With this choice, $S_s = 0$ and $\rho_L = 0$.

The departing noise wave B_2 at the output becomes by inspecting Fig. 3(b)

$$B_2 = B_{q2} + \frac{S_{22}^0 S_{21}}{1 - S_{22}^0 S_{11}} B_{q1} + \frac{S_{21}^0 S_{21}}{1 - S_{22}^0 S_{11}} B_{qs}. \tag{16}$$

It is advantageous to introduce the linear transformations

$$B_{q1} = S_{11} B_{i2} + B_{i1} \tag{17a}$$

$$B_{q2} = S_{21} B_{i2} \tag{17b}$$

into (16), thus referring the noise wave B_2 to equivalent noise sources at the input of the noisy two-port. With this step, which is analogous to the procedure developed in [1], one obtains a simple relation showing more clearly the interaction between the noisy two-port and the matching network

$$B_2 = \frac{S_{21}}{1 - S_{22}^0 S_{11}} \left[S_{22}^0 B_{i1} + B_{i2} + S_{21}^0 B_{qs} \right]. \tag{18}$$

It is obvious that the newly defined, equivalent noise sources, B_{i1} and B_{i2}, also are, in general, correlated (as are B_{q1} and B_{q2}). Therefore, it is principally possible to minimize their contribution by properly adjusting S_{22}^0 of the input matching network. This is conveniently shown by means of the noise factor. Since the available noise power is given by

$$p_2 = \tfrac{1}{2} E\{B_2 B_2^*\}$$

the noise factor F as defined in [6] becomes, in terms of (18),

$$F = 1 + \frac{E\{B_{i2} B_{i2}^*\} + S_{22}^0 S_{22}^{0*} E\{B_{i1} B_{i1}^*\} + S_{22}^0 E\{B_{i1} B_{i2}^*\} + S_{22}^{0*} E\{B_{i1}^* B_{i2}\}}{S_{21}^0 S_{21}^{0*} E\{B_{qs} B_{qs}^*\}}. \tag{19}$$

[2]The assumption made here of a "cold" load impedance is not necessary. However, it simplifies the argument considerably.

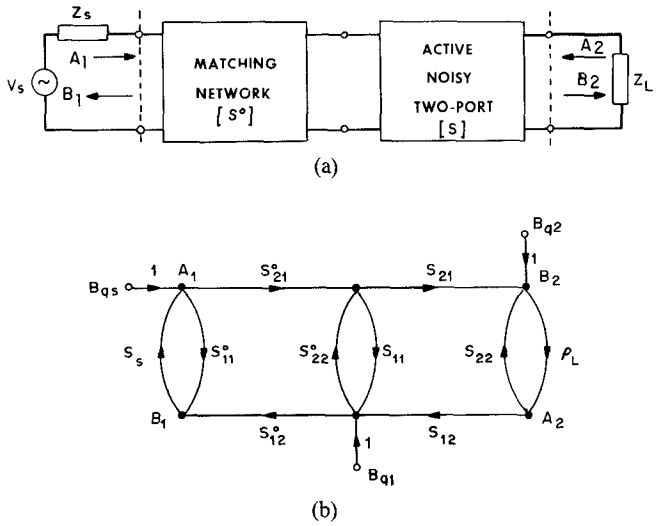

Fig. 3. Noise matching of an active linear two-port. (a) Block diagram. (b) Associated signal flowgraphs.

This expression can be simplified by introducing the normalized quantities

$$q_1 = \frac{E\{B_{i1} B_{i1}^*\}}{E\{B_{qs} B_{qs}^*\}} \tag{20a}$$

and

$$q_2 = \frac{E\{B_{i2} B_{i2}^*\}}{E\{B_{qs} B_{qs}^*\}}. \tag{20b}$$

The cross-correlation terms $E\{B_{i1} B_{i2}^*\}$ and $E\{B_{i1}^* B_{i2}\}$ will be replaced by introducing the complex cross-correlation factor

$$\Gamma_{12} = \frac{E\{B_{i1} B_{i2}^*\}}{\sqrt{E\{B_{i1} B_{i1}^*\} E\{B_{i2} B_{i2}^*\}}}. \tag{21}$$

With (20a), (20b), and (21) the noise factor becomes

$$F = 1 + \frac{S_{22}^0 S_{22}^{0*} q_1 + q_2 + \sqrt{q_1 q_2} \left(\Gamma_{12} S_{22}^0 + \Gamma_{12}^* S_{22}^{0*} \right)}{1 - S_{22}^0 S_{22}^{0*}}. \tag{22}$$

Note that we made use of the condition $S_{21}^0 S_{21}^{0*} = 1 - S_{22}^0 S_{22}^{0*}$ assuming that the matching network is lossless. The nonnegative, real parameters q_1 and q_2 and the complex correlation factor Γ_{12} are inherent to the noisy two-port. They are characteristic of the noise behavior and have, therefore, fundamental importance.

VI. Circles of Constant Noise Factors

In the following, we will show that (22) defines the familiar circles of constant noise factors [8] in the complex plane of the output reflection coefficient S_{22}^0. For convenience we introduce the "excess" noise factor $F_z = F - 1$ and

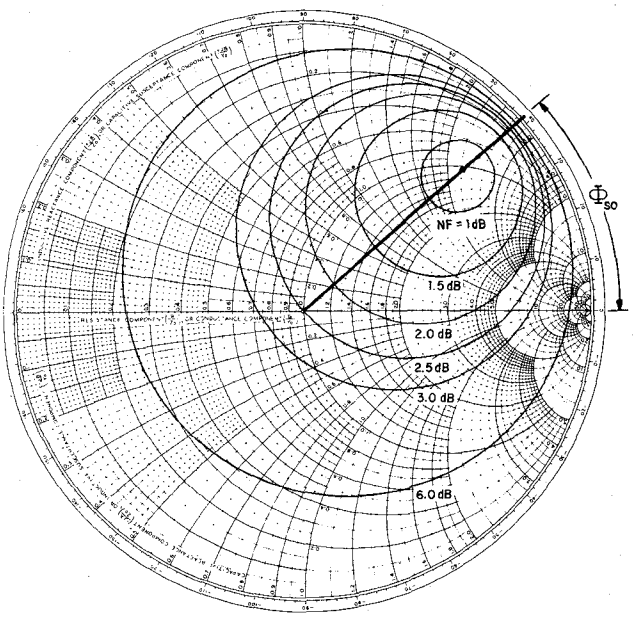

Fig. 4. Circles of constant noise figure.

rearrange (22) as follows:

$$S_{22}^0 S_{22}^{0*} + Q^* S_{22}^{0*} + Q S_{22}^0 = M \tag{23}$$

where the complex quantity Q and the real value M stand for

$$Q = \Gamma_{12} \frac{\sqrt{q_1 q_2}}{F_z + q_1} \tag{24}$$

$$M = \frac{F_z - q_2}{F_z + q_1}. \tag{25}$$

Equation (23) can also be written in the form

$$\left(S_{22}^0 + Q^*\right)\left(S_{22}^0 + Q^*\right)^* = M + |Q|^2 \tag{26}$$

from which the desired result immediately follows:

$$S_{22}^0 = -Q^* + \sqrt{M + |Q|^2}\, e^{j\psi} \tag{27}$$

with ψ being an arbitrary angle. Equation (27) defines the location and radius of a family of circles in the plane of S_{22}^0 which are solely dependent on the given noise factor F and the characteristic noise parameters of the two-port. The centers of these circles are located at $S_{22}^0 = -Q^*$ and their radii are given with $\sqrt{M + |Q|^2}$. Examples are shown in Fig. 4 with the noise figure (NF) being the noise factor in decibels (i.e., NF $= 10 \log F$).

VII. The Optimum Noise Factor

The lowest, optimum noise factor F_{opt} (or $F_{z\text{opt}} = F_{\text{opt}} - 1$) is conveniently found by using a complex phasor notation for S_{22}^0 and Γ_{12}

$$S_{22}^0 = m e^{j\Phi_s}, \qquad 0 \leq m \leq 1$$

$$\Gamma_{12} = r e^{j\Phi_r}, \qquad 0 \leq r \leq 1.$$

Then, (22) becomes

$$F_z = \frac{m^2 q_1 + q_2 + 2\sqrt{q_1 q_2}\, mr \cos\left(\Phi_r + \Phi_s\right)}{1 - m^2}. \tag{28}$$

Minima of F_z with respect to Φ_s are obtained when $\Phi_r + \Phi_s = (2\lambda + 1)\pi$, with $\lambda = 0, 1, 2 \cdots$. Thus for $\Phi_s = \Phi_{s0} = (2\lambda + 1)\pi - \Phi_r$, F_z becomes

$$F_{z\min} = \frac{m^2 q_1 + q_2 - 2\sqrt{q_1 q_2}\, mr}{1 - m^2}. \tag{28a}$$

It is easy to see that $F_{z\min}$ has an absolute minimum value ($F_{z\text{opt}}$) as function of m: differentiating $F_{z\min}$ with respect to m and equating the differential to zero will lead to the condition for a value of m for which $F_{z\min}$ becomes optimum. Denoting this value of m as m_0, one finds after some algebra

$$m_0 = u - \sqrt{u^2 - 1} \tag{29}$$

where the auxiliary quantity u is defined by

$$u = \frac{1}{2r} \frac{q_2 + q_1}{\sqrt{q_2 q_1}} \tag{30}$$

provided r, q_1, and q_2 are nonzero. Note that m_0 is solely dependent on the scalar values r, q_1, and q_2. $F_{z\text{opt}}$ is determined by

$$\left(F_{z\text{opt}} - q_2\right)\left(F_{z\text{opt}} + q_1\right) + r^2 q_1 q_2 = 0 \tag{31}$$

or explicitly

$$F_{z\text{opt}} = \frac{1}{2}\left[\left(q_2 - q_1\right) + \left(q_1 + q_2\right)\frac{\sqrt{u^2 - 1}}{u}\right] \tag{31a}$$

with u given by (30).

It can be shown that $F_{z\text{opt}}$ can also be expressed in the more compact forms

$$F_{z\text{opt}} = \frac{r\sqrt{q_1 q_2}}{m_0} - q_1 \tag{31b}$$

or

$$F_{z\text{opt}} = q_2 - m_0 r \sqrt{q_1 q_2}. \tag{31c}$$

Equation (31) is a direct proof of the property that the radius of the circle for the optimum noise figure is zero. To show this, one only has to equate $\sqrt{M + |Q|^2}$ to zero and set $F_z = F_{z\text{opt}}$, whence (31) follows. Interestingly, at this optimum value, (24) leads to (31b) by recalling that $m_0 = |S_{22}^0|_{\text{opt}} = |Q|$ for $F_z = F_{z\text{opt}}$.

VIII. The Measurement of the Characteristic Noise Parameters

The measurement of the noise wave parameters is easily accomplished with the use of a noise factor measuring set and a lossless matching network with adjustable reflection coefficient (e.g., double slug tuner) at the input of the device under test.

With the input terminated in the characteristic impedance ($Z_s = Z$) one has $m = 0$, whence from (28)

$$q_2 = F_{z0} = F_z(m = 0). \tag{32}$$

Besides being obvious, this result is noteworthy because it states that the characteristic noise parameter q_2 is identical with the excess noise factor obtained with the ordinary resistive termination at the input. In the next measurement, one determines with $m \neq 0$ the angle Φ_{s0} for which F_z

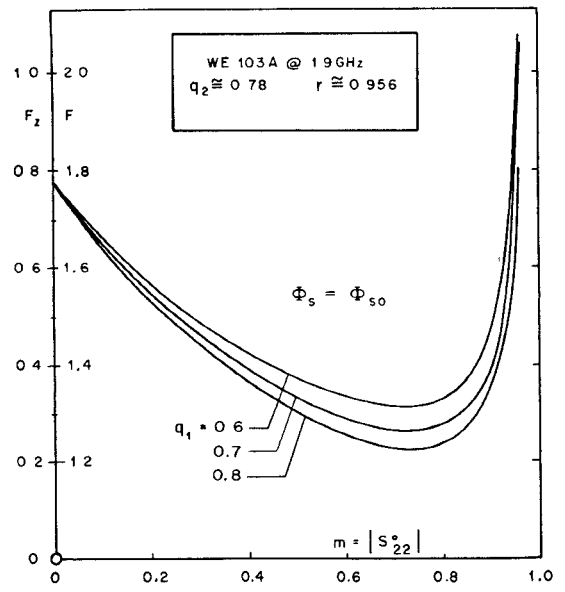

Fig. 5. Noise factor versus magnitude of S^0_{22}.

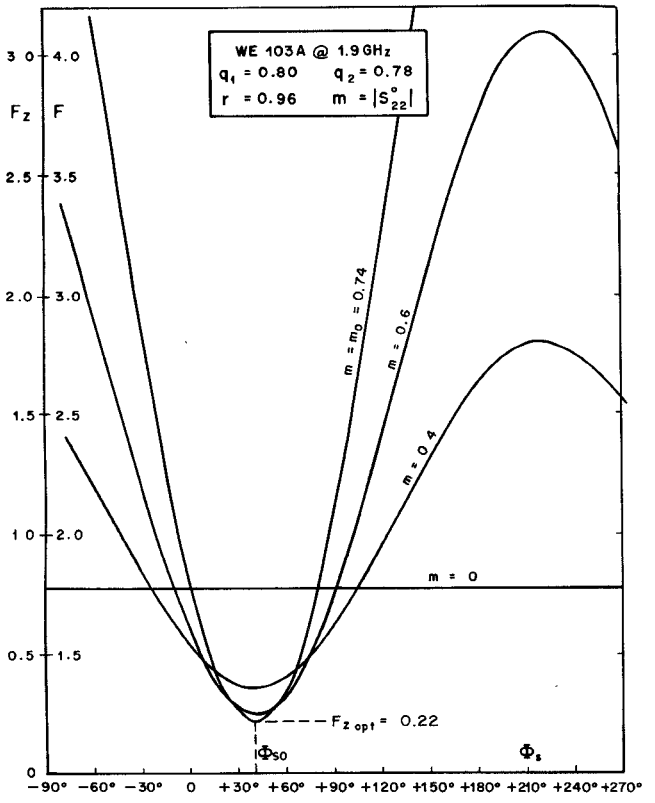

Fig. 6. Noise factor versus phase of S^0_{22}.

becomes $F_{z\min}$ and then m_0 (keeping $\Phi_s = \Phi_{s0}$ constant) for which $F_{z\min}$ becomes $F_{z\text{opt}}$. With the two results (m_0 and $F_{z\text{opt}}$) obtained and q_2 already determined, one computes q_1 and r from

$$q_1 = \frac{q_2 - F_{z\text{opt}}}{m_0^2} - F_{z\text{opt}} \tag{33}$$

$$r = \frac{q_1 + q_2}{\sqrt{q_1 q_2}} \cdot \frac{m_0}{1 + m_0^2}. \tag{34}$$

If required, Φ_r is found from $\Phi_r = \pi - \Phi_{s0}$. It must be noted that the parameter q_1 is sensitive in regard to the accuracy in measuring m_0, the optimum magnitude of the reflection coefficient. Unfortunately, the minimum of F_z as function of m is not sharply defined allowing for a potentially large error in determining m_0. This is best illustrated by computing and plotting F_z versus m according to (28), as shown in Fig. 5, with Φ_s, q_2, and r being kept constant and q_1 deliberately being varied. As is seen, for any given q_1, the noise factor attains its minimum within 0.012, corresponding to a variation of 0.05 dB, over a substantial range of m. (This is, of course, an advantage for the designer because it allows for a larger margin in realizing the required matching network.) The magnitude of the correlation factor r is considerably less sensitive to errors in m_0. Typically, low-noise GaAs FET's (WE type 103) measured at 2 GHz exhibit values of q_1 between 0.6 and 0.8; the other parameters determined for this device are $q_2 = 0.78$ and $r = 0.96$, as shown on Fig. 5. The optimum phase angle also has a fairly broad minimum as is seen from Fig. 6 showing the vibration of F_z as function of the phase of S^0_{22} with m as a parameter.

IX. Lossy Matching Networks

Equation (22) made use of the "lossless" condition $S^0_{21}S^{0*}_{21} = 1 - S^0_{22}S^{0*}_{22}$ of the matching network. However, in most applications this is not true at microwave frequencies because of losses due to dissipation and radiation. As shown in the Appendix, one can account for these losses by introducing the dissipation factor

$$d_2^2 = 1 - \left(S^0_{21}S^{0*}_{21} + S^0_{22}S^{0*}_{22}\right). \tag{35}$$

Obviously, $0 \leq d_2^2 \leq 1$; $d_2^2 = 0$ corresponds to the lossless case. The internal dissipation losses of the matching network indicate the existence of thermal noise which must be accounted for by adding independent noise sources as depicted in the signal flowgraph of Fig. 7 (B_{s1} and B_{s2}). In the Appendix it is shown that these sources have the magnitude

$$|B_{s1}| = d_1\sqrt{2kT_N\Delta f} \text{ and } |B_{s2}| = d_2\sqrt{2kT_N\Delta f}$$

with d_1 defined similar to (35) and T_N being the absolute temperature of the matching network. Compared to (18), the departing noise wave at the output then becomes

$$B_2 = \frac{S_{21}}{1 - S^0_{22}S_{11}}\left(B_{i2} + S^0_{22}B_{i1} + S^0_{21}B_{qs} + B_{s2}\right). \tag{36}$$

Under the assumption that the lossy network is at standard temperature ($T_N = T_0$) and applying the same procedures as outlined in Section V, the excess noise factor is now derived as

$$F_z = \frac{d_2^2 + m^2q_1 + q_2 + 2\sqrt{q_1q_2}\,mr\cos\left(\Phi_r + \Phi_s\right)}{1 - d_2^2 - m^2}. \tag{37}$$

Note that the noise factor of the lossy matching network alone can be computed from (37) by setting q_1, q_2, and r to zero:

$$F_{\text{network}} = F_z + 1 = \frac{1 - m^2}{1 - d_2^2 - m^2}.$$

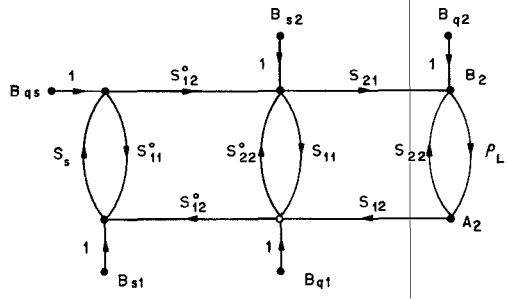

Fig. 7. Signal flowgraph of cascade of lossy noise matching network and active two-port.

TABLE I
CHARACTERISTIC NOISE PARAMETERS (WE 103A GaAs FET at 2 GHz)

$d_2^2 = 0$ (D.L. = 0 dB)	$d_2^2 = 0.056$ (D.L. = 0.25 dB)
$q_1 = 0.722$	$q_1 = 0.660$
$q_2 = 0.862$	$q_2 = 0.756$
$r = 0.923$	$r = 0.972$

This is a well-known result for $m=0$.

It is seen from (37) that the measurement of F_z, in the presence of dissipative losses in the matching circuit, will lead to different values of the noise parameters. In place of (32)–(34) one finds the new set

$$q_2 = F_{z0}\left(1-d_2^2\right)-d_2^2 \tag{38}$$

$$q_1 = \frac{\left(1-d_2^2\right)\left(F_{z0}-F_{z\,\mathrm{opt}}\right)}{m_0^2} - F_{z\,\mathrm{opt}} \tag{39}$$

and

$$r = \frac{d_2^2+\left(1-d_2^2\right)q_1+q_2}{\sqrt{q_1 q_2}} \cdot \frac{m_0}{1-d_2^2+m_0^2} \tag{40}$$

where F_{z0}, $F_{z\,\mathrm{opt}}$, and m_0 are defined as before.

A numerical example will illustrate the effect of these changes. A WE 103A low-noise GaAsFET was matched at about 2 GHz for minimum noise figure using a matching network with 0.25-dB dissipation loss; i.e., $d_2^2=0.056$. The minimum noise figure was found to be $\mathrm{NF}_{\mathrm{opt}}=1.4$ dB ($F_{z\,\mathrm{opt}}=0.38$) for $m_0=|S_{22}^0|=0.66$. With a matched source, the noise figure was 2.70 dB ($F_{z0}=0.86$). Table I compares the values of the noise parameters calculated from (38)–(40) (lossy case) to those obtained with (32)–(34) (lossless case). As one might expect, the parameters q_1 and q_2 decrease if one accounts for losses while the correlation between them (r) increases. If this same device could be matched with a perfectly lossless circuit, its optimum matching reflection coefficient as calculated with (29) and (30) would be $m_0=0.78$. The corresponding optimum noise figure computed from (31a) becomes $\mathrm{NF}_{\mathrm{opt}}=0.87$ dB. This is to be compared with the measured value of 1.4 dB. Simply subtracting 0.25-dB dissipation loss from 1.4 dB would still leave a substantial error of almost 0.3 dB. It is essential, therefore, to carefully account for dissipative losses in matching circuits when evaluating and characterizing very low-noise devices.

X. Conclusion and Summary

It is shown how noise as a stationary stochastic process can be approximated by an infinite series of scattered waves. Each partial wave represents spot noise. Therefore, the scattering matrix formalism as well as signal flow graph analysis for linear networks and systems can be extended to include the analysis of spot noise. The noise waves lead to a new set of characteristic noise parameters of noisy two-ports. These parameters are based on the inherent noise waves which emanate from each port and which correspond directly to the available noise power and their cross correlation.

With these parameters, the theory of minimizing amplifier noise by noise matching is straightforward, and the definition of circles of constant noise figure in the Smith Chart is simple. The effect of lossy matching networks on the noise figure of amplifiers is shown to be more significant for typical low-noise microwave GaAsFET's than ordinarily assumed.

Appendix

Thermal Noise From Passive Lossy Two-Ports

A linear, reciprocal, and lossy two-port can be represented by a passive network of ideal *RLC* elements. Obviously, all losses are then caused by the discrete resistors. This being the case, each resistor will, in general, cause thermal noise to appear at all ports. As indicated in Fig. 8, one can visualize these resistors to be connected to extra ports such that the resulting network, exclusive of the resistors, is lossless. The resistor R_j at the jth port is the source of a spot noise wave which according to (10) has the magnitude

$$|B_{qj}| = \sqrt{\left(1-|\rho_j|^2\right)} \cdot \sqrt{2kT_j\Delta f}$$

where ρ_j stands for $(R_j-Z)/(R_j+Z)$ in accordance with (8). Thus with N sources in the network, the first two scattering wave equations can be written as follows:

$$B_1 = S_{11}A_1 + S_{12}A_2 + \sum_{j=3}^{N+2} S_{1j}\sqrt{1-|\rho_j|^2} \cdot \sqrt{2kT_j\Delta f}$$

$$B_2 = S_{21}A_1 + S_{22}A_2 + \sum_{j=3}^{N+2} S_{2j}\sqrt{1-|\rho j|^2} \cdot \sqrt{2kT_j\Delta f}. \tag{A1}$$

Because the internal source waves are uncorrelated, the noise power in the departing waves due to the internal sources only is then

$$\tfrac{1}{2}E\{B_1B_1^*\} = \sum_{j=3}^{N+2} |S_{1j}|^2\left(1-|\rho_j|^2\right)\cdot kT_j\Delta f$$

$$\tfrac{1}{2}E\{B_2B_2^*\} = \sum_{j=3}^{N+2} |S_{2j}|^2\left(1-|\rho_j|^2\right)\cdot kT_j\Delta f.$$

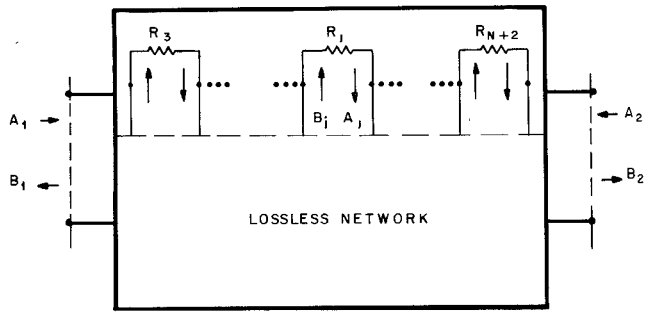

Fig. 8. Partitioning of a lossy two-port into a lossless network and N resistive terminations.

Obviously, for noise power calculations the phases of S_{1j} and S_{2j} are irrelevant and (A1) can also be expressed as

$$B_1 = S_{11}A_1 + S_{12}A_2 + \sqrt{\sum_{j=3}^{N+2} |S_{1j}|^2 \left(1-|\rho_j|^2\right) 2kT_j\Delta f}$$

$$B_2 = S_{21}S_1 + S_{22}A_2 + \sqrt{\sum_{j=3}^{N+2} |S_{2j}|^2 \left(1-|\rho_j|^2\right) 2kT_j\Delta f}. \quad \text{(A2)}$$

If the temperature within the network is uniform, i.e., if all resistors R_j are at the same temperature T_N, *and* since we assumed reciprocity, i.e., $S_{ij}=S_{ji}$, (A2) can be simplified significantly:

$$B_1 = S_{11}A_1 + S_{12}A_2 + \sqrt{1-|S_{11}|^2-|S_{12}|^2}\cdot\sqrt{2kT_N\Delta f}$$

$$B_2 = S_{12}A_1 + S_{22}S_2 + \sqrt{1-|S_{12}|^2-|S_{22}|^2}\cdot\sqrt{2kT_N\Delta f}. \quad \text{(A3)}$$

To prove the validity of (A3), we apply sinusoidal signals to port 1 and port 2 and compute that portion of the power from these signals which is dissipated in the jth resistor

$$p_{dj} = \tfrac{1}{2}E\{B_jB_j^*\} - \tfrac{1}{2}E\{A_jA_j^*\} = \tfrac{1}{2}|B_j|^2 - \tfrac{1}{2}|A_j|^2.$$

Because $A_j = \rho_j B_j$, this becomes

$$p_{dj} = \tfrac{1}{2}|B_j|^2\left(1-|\rho_j|^2\right).$$

B_j, however, is related to the incident waves A_1 and A_2 through

$$B_j = S_{j1}A_1 + S_{j2}A_2$$

whence

$$p_{dj} = |S_{j1}|^2\left(1-|\rho_j|^2\right)\tfrac{1}{2}|A_1|^2 + |S_{j2}|^2\left(1-|\rho_j|^2\right)\tfrac{1}{2}|A_2|^2.$$

The total power dissipated in the N resistors is then simply

$$p_d = \sum_{j=3}^{N+2}\left\{|S_{j1}|^2\left(1-|\rho_j|^2\right)\right\}\tfrac{1}{2}|A_1|^2 + \sum_{j=3}^{N+2}\left\{|S_{j2}|^2\left(1-|\rho_j|^2\right)\right\}\tfrac{1}{2}|A_2|^2. \quad \text{(A4)}$$

This power must be equal to the total power incident less the total power departing:

$$p_d = \tfrac{1}{2}\left(|A_1|^2 + |A_2|^2 - |B_1|^2 - |B_2|^2\right).$$

Using (A1) this yields for the sinusoidal waves

$$p_d = \left(1-|S_{11}|^2-|S_{12}|^2\right)\tfrac{1}{2}|A_1|^2 + \left(1-|S_{21}|^2-|S_{22}|^2\right)\tfrac{1}{2}|A_2|^2. \quad \text{(A5)}$$

Thus with $S_{ij}=S_{ji}$ and by comparing (A4) and (A5), we find

$$\sum_{j=3}^{N+2} |S_{1j}|^2\left(1-|\rho_j|^2\right) = 1-|S_{11}|^2-|S_{12}|^2$$

and

$$\sum_{j=3}^{N+2} |S_{2j}|^2\left(1-|\rho_j|^2\right) = 1-|S_{12}|^2-|S_{22}|^2.$$

With this result the proof of (A3) is complete.

It is convenient to use in (A3) the abbreviations

$$d_1 = \sqrt{1-|S_{11}|^2-|S_{12}|^2}$$

and

$$d_2 = \sqrt{1-|S_{12}|^2-|S_{22}|^2}.$$

These quantities may be computed from known dissipation losses using the definition

$$\mathrm{DL} = -10\log\left(1-d^2\right)\mathrm{dB}.$$

Note that the dissipation losses depend on the direction of transmission. With d_1 and d_2 defined, (A3) becomes

$$B_1 = S_{11}A_1 + S_{12}A_2 + d_1\sqrt{2kT_N\Delta f}$$

$$B_2 = S_{12}A_1 + S_{22}A_2 + d_2\sqrt{2kT_N\Delta f}. \quad \text{(A6)}$$

Using (A6) in a spot noise analysis one can correctly account for thermal noise from linear, reciprocal, and lossy two-ports provided the temperature within is uniform and known.

Acknowledgment

The author is grateful to R. W. Judkins for his noise measurements and to J. J. Daly and J. E. Knecht for valuable discussions and contributions to this subject.

References

[1] H. Rothe and W. Dahlke, "Theorie Rauschender Vierpole," *Arch. Elek. Übertragung*, vol. 9, pp. 117–121, 1955.

[2] H. Bauer and H. Rothe, "Der Aquivalente Rauschvierpol als Wellenvierpol," vol. 10, pp. 241–252, 1956.

[3] P. Penfield, "Wave representation of amplifier noise," *IRE Trans. Circuit Theory*, vol. CT-9, p. 84, Mar. 1962.

[4] R. P. Meys, "A wave approach to the noise properties of linear microwave devices," *IEEE Trans. Microwave Theory Tech.*, vol. MTT-26, pp. 34–37, Jan. 1978.

[5] A. Papoulis, *Probability, Random Variables, and Stochastic Processes*. New York: McGraw-Hill, 1955.

[6] H. A. Haus *et al.*, Noise in Linear Two-ports, "IRE standards on electron tubes: methods of testing," 62 IRE7 S1, pt. 9, 1962.

[7] H. A. Haus and R. B. Adler, "Invariants of linear noisy networks," *IRE Conn. Rec.*, pt. 2, p. 53, 1956.

[8] H. Fukui, "Available power gain, noise figure, and noise measure of two-ports and their graphical representations," *IEEE Trans. Circuit Theory*, vol. CT-13, p. 137, June. 1966.

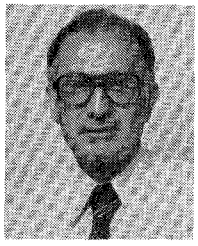

Rudolf P. Hecken was born in Bad Hönningen, Rhein, Germany. He received the diploma in electrical engineering in 1959, and the Ph.D. degree in 1964, both from the Technische Hochschule Aachen, Germany.

While at the High-Frequency Institute at Aachen, Germany, he was engaged in teaching and research on pulse techniques between 1959 and 1962. From 1962 to 1965 he worked at the same Institute on the development of He–Ne gas lasers. In 1965 he joined the European Center for Nuclear Research (CERN) where he investigated new RF accelerating methods for a high-energy synchro-cyclotron. From 1968 until 1973 he was employed by Bell Telephone Laboratories, North Andover, MA, where he was engaged in the development of millimeter wave components and other transmission systems networks and components. After going to Germany for one year, he returned to the Bell Laboratories, North Andover, MA, in 1974, and became responsible for design and development of the transmitter of the AR 6A SSB microwave radio system. Currently, he heads a department engaged in exploratory studies on digital radio systems. He holds several patents and has published seven papers.

Performance of Optically Coupled Microwave Switching Devices

RICHARD A. KIEHL, MEMBER, IEEE, AND DAVID M. DRURY MEMBER, IEEE

Abstract—**The performance of optically coupled microwave switching devices for pulse generation or other applications is detailed. The bias dependence of the RF power transfer is presented for a range of operating frequencies, thereby establishing the bias conditions required for a given ON/OFF ratio and insertion loss. Limits on peak RF power level and pulse repetition rate, as well as limitations arising from harmonic distortion and shot noise, are also examined.**

I. INTRODUCTION

THE RECENT EMERGENCE of solid-state optical device technology has made possible new microwave devices that are hybrids of conventional microwave technology and the newer optical technology. For the most part, such devices proposed to date use lightwaves to control the behavior or regulate the characteristics of some microwave element, be it an oscillator [1], [2], a switch [3], [4], or some other microwave device [5]. However, one can also envision a new class of microwave components wherein lightwaves are used not for control, but rather for the coupling of microwave energy from one point to another. Thus lightwaves would be used in a fashion analogous to that of the "opto-isolator" employed in lower frequency circuitry for some time.

Manuscript received October 29, 1980; revised April 10, 1981. This work was supported by the U.S. Department of Energy (D.O.E.) under Contract DE-AC04-76-DP00789.

R. A. Kiehl was with Sandia National Laboratories, Alburquerque, NM. He is now with Bell Laboratories, Murray Hill, NJ 07974.

D. M. Drury is with Sandia National Laboratories, Alburquerque, NM 87185.

A component of this type was recently proposed by MacDonald and Hara [6], [7] for use as the crosspoint element in a video-signal switching array. The switch was based on the detector-bias dependence of the coupling between an optical source/detector pair. A very attractive feature of this switch for such RF signal routing is that it confines the RF energy to a narrow optical path. This allows the achievement of nearly zero signal cross-coupling even in highly compact switching arrays.

Independent of this work, we proposed [8] the same switching concept as the basis of a microwave gate for pulse generation and other applications. Here, the attractiveness of the switch results from its extremely high ON/OFF ratio and reverse isolation, as well as from the fact that its input impedance is completely independent of switching state. In pulse radar applications where a switch is used to gate a microwave source, for example, a high ON/OFF ratio and a high reverse isolation can lead to improvements in sensitivity and jamming immunity. A state-independent input impedence means that the problem of oscillator "pulling" is eliminated, which is crucial in phase-sensitive radar designs.

In the present paper, we report experimental results on the performance of such optically coupled microwave switches relevant to a variety of applications. We begin in Section II by considering RF power-transfer capability which determines the ultimate insertion loss of the switch. In Section III, we examine the ON/OFF ratio achievable under various operating conditions. Section IV deals with

0018-9480/81/1000-1004$00.75 ©1981 IEEE